Dynamically modulated perfect absorbers

Suwun Suwunnarat, Dashiell Halpern, Huanan Li, Boris Shapiro, and Tsampikos Kottos

Phys. Rev. A **99**, 013834 — Published 22 January 2019

DOI: 10.1103/PhysRevA.99.013834

Dynamically Modulated Perfect Absorbers

Suwun Suwunnarat[1], Dashiell Halpern[1], Huanan Li[1*], Boris Shapiro[2†], Tsampikos Kottos[1‡]
[1] *Wave Transport in Complex Systems Lab, Department of Physics, Wesleyan University, Middletown, CT-06459, USA and*
[2] *Technion - Israel Institute of Technology, Technion City, Haifa 32000, Israel*
(Dated: January 2, 2019)

We introduce the concept of multichannel Dynamically Modulated Perfect Absorbers (DMPAs) which are periodically modulated lossy interferometric traps that completely absorb incident monochromatic waves. The proposed DMPA protocols utilize a Floquet engineering approach which inflicts a variety of emerging phenomena and features: *reconfigurability* of perfect absorption (PA) for a broad range of frequencies of the incident wave; PA for infinitesimal local losses, and PA via critical coupling with high-Q modes by inducing back-reflection *dynamical* mirrors.

PACS numbers: 05.45.-a, 42.25.Bs, 11.30.Er

I. INTRODUCTION

The quest of new methods and technologies that can lead to a perfect absorption (PA) of an incident waveform is an interdisciplinary research theme in classical wave physics. It spans a range of frequencies from optics[1–13] and microwaves[14–17], to radio-frequencies[18,19], acoustics[20–23] and electronics[24–26]. A successful outcome can revolutionize a variety of wave physics applications including energy conversion[27,28] and photovoltaics[29–31], imaging techniques[32–35] and medical therapies[36], stealth technologies[19,37,38] and soundproofing[23,39].

A desirable feature for many of the above applications is an "on-the-fly" reconfigurability of the structure i.e. the possibility to absorb on demand an incoming monochromatic wave at a specific frequency, without altering the fabrication characteristics of the structure itself. Another requirement, either due to cost or design considerations, is to incorporate minimal losses inside the structures while at the same time achieve a perfect absorption. This second requirement has been recently addressed, in the frame of multi-channel systems, by the so-called *Coherent Perfect Absorber* (CPA) scheme. This is an interferometric protocol employing two counter-propagating waves which destructively interfere outside a weakly lossy cavity (the target)– in analogous manner to time-reversed laser - to achieve coherent perfect absorption[3,5]. The original concept, involving only two channels coupled to a simple cavity has been realized in various frameworks[5,13,26,40] and further extended to include multi- channel complex cavities[41–43]. CPA is a "generalization" of an older scheme, applicable only for single-channel cavities, which employs a back-reflection mirror and *critical coupling* to the resonances of the lossy cavity. Unfortunately, two (or multi) -sided coherent wave injection in some applications might be challenging to implement, while back-reflection mirrors are often either lossy (e.g. metallic mirrors) or require additional fabrication effort (e.g. distributed Bragg reflectors). To make things worst, none of the above proposals addresses the "on-the-fly" reconfigurability issue. Along these lines, the recent work[44] stands out, since it is the first one that proposes to use parametric amplification for the implementation of reconfigurable CPAs. This approach requires periodic modulation of the refractive index at frequencies which are twice the frequency of the incident signal – thus imposing some limitations, specifically in the optical domain. Obviously, a more flexible scheme is extremely desirable.

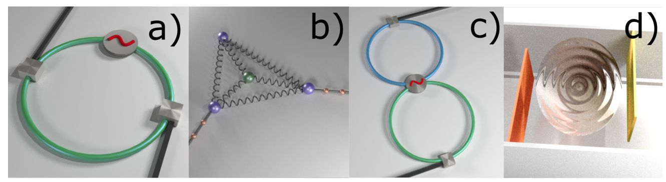

Figure 1: (Color Online) Schematics of various physical setups that can be used for DMPA: (a) A single-mode fiber coupled to a time-periodic phase modulator; (b) A network of four oscillators (resonators) with modulated coupling constants; (c) Two single-mode fibers with a time- modulated coupler; and (d) an acoustic cavity with two cantilevers where the in-between air domain is periodically modulated in time. Weakly lossy elements are indicated with green.

In this paper we introduce PA in a completely different framework associated with Floquet time-modulated systems. The latter has gain in recent years a lot of momentum– specifically in connection with non-reciprocal transport[45–48] Here, using a Floquet scattering formalism we show that the proposed *Dynamically Modulated Perfect Absorber* (DMPA) protocols are "on-the-fly" reconfigurable and can PA any specified frequency of the incoming waves by altering the external driving characteristics – a feature that is absent from any static PA scheme whose properties are fixed during the fabrication process. Importantly, we show that the implementation of Floquet engineering methods provide powerful means

*hli01@wesleyan.edu
†boris@physics.technion.ac.il
‡tkottos@wesleyan.edu

for the implementation of PA protocols with unconventional characteristics. For example, we demonstrate perfect absorption via coherent multi-channel illumination for *infinitesimal local* losses – a phenomenon which we refer to as *Floquet-enhanced perfect absorption* – occurring at appropriate values of the frequency/ amplitude of the periodic driving scheme. Finally, we show that our scheme can be flexible and interpolate between coherent DMPA and PA via critical coupling associated with single-channel illumination. We demonstrate that the latter scenario can occur even in the absence of physical back-reflecting mirrors. The latter is induced dynamically via Floquet engineering.

The structure of the paper is as follows. In the next section II we present the theoretical model which is based on coupled mode theory. We also derive the associated Floquet scattering matrix and identify conditions under which our formalism is applicable. In section III we derive the necessary conditions for perfect absorption in the case of dynamically modulated targets. Moreover, we theoretically derive expressions for the incident frequency and loss-strength for which perfect absorption occurs. In section IV we discuss the case of DMPA for coherent incident waves. Specific examples are analyzed in detail – both theoretically and numerically. In section V we analyze the scenario where DMPA is induced via dynamical mirrors imposed to the system due to the Floquet driving. Finally our conclusions are presented at the last section VI. At the Appendix we provide some details associated with the numerical models that have been used to demonstrate DMPA in the text.

II. FLOQUET SCATTERING FORMALISM

We consider a cavity, or a network of N_s coupled single-mode cavities. Hereafter we refer to the cavities as "sites" with the corresponding resonant mode attached to each site. The mode frequencies, and generally the couplings, are periodically modulated by an electric field which is periodic in time with period $T = 2\pi/\omega$. For some physical set-ups see Fig. 1. In the context of coupled-mode theory, the time-periodic Floquet resonator network can be described by an effective time-periodic Hamiltonian $H(t) = H(t + 2\pi/\omega)$ which takes the form

$$H(t) = H_0(t) - \imath\Gamma, \quad \Gamma = \sum_{\mu} \gamma_\mu |e_\mu\rangle \langle e_\mu| . \qquad (1)$$

Above $H_0(t)$ is a $N_s \times N_s$ Hermitian matrix, γ_μ quantifies the loss in the μ-th cavity and $\{|e_\mu\rangle\}$ is the basis of the mode space where $H_0(t)$ is represented. We turn the system of Eq. (1) to a scattering set-up by attaching to it two static semi-infinite leads $\alpha = L, R$, each of which is supporting plane waves with a dispersion relation $\Omega(k)$. We shall assume, for demonstration purposes, that the leads consist of an one-dimensional array of coupled resonators. We further assume that we can identify in each of these resonators one well isolated high-Q resonant mode. Under these assumptions the leads can be described by an one-dimensional tight-binding dispersion $\Omega = -2C\cos(kx_0)$ where x_0 represents the distance between the resonators. The constant C represents the coupling strength between the sites of the tight-binding elements of the leads and controls the band-width of the propagating channels. We emphasis that around the center of the band i.e. $kx_0 \approx \pi/2$ the tight-binding dispersion will be reduce to the free-space like dispersion under the wide-band approximation[49]. Specifically, we will have that $\Omega \approx 2Cx_0k$. In this case, and for relatively small driving frequency compared with the band-width, our discussion below will be also applicable to the study of DMPA in the free space. Below we will adopt a natural unit system by setting $C = x_0 = 1$. The loss strength of the lossy resonator(s) are assumed to be the same $\gamma_\mu = \gamma$.

When an incident wave with frequency $\Omega_0 = \Omega(k_0) \in [-\omega/2, \omega/2]$ is engaged with the periodically-modulated target, it is scattered to an infinite number of outgoing channels (including evanescent ones) supporting frequencies $\Omega_n = \Omega_0 + n\omega = -2\cos k_n$ (n is an integer). The evanescent channels (that are supported in the semi-infinite leads) with $\Omega_n \notin (-2, 2)\,, \mathrm{Im}k_n > 0$ do not carry flux. We, therefore, consider the scattering matrix $\mathcal{S}$ which connects only the N_p incoming with the outgoing propagating channels $\Omega_n \in (-2, 2)\,, k_n \in (0, \pi)$ at each of the $\alpha = L, R$ leads. Following Ref.[48] we write the flux-normalized scattering matrix S as

$$\mathcal{S} = -I_{2N_p} + \imath W G_s W^T, G_s \equiv \frac{1}{\Omega_0 - H_Q + W_c^T K W_c} \qquad (2)$$

where I_{2N_p} is the $2N_p \times 2N_p$ identity matrix. The quasi-energy operator H_Q is defined in the Floquet-Hilbert space and has elements $(H_Q)_{ns,n's'} = H_{ss'}^{(n-n')} - \delta_{nn'} n\omega$ where the Fourier components are $H_{ss'}^{(n)} \equiv \frac{1}{T}\int_0^T dt H_{ss'}(t) \exp(\imath n\omega t)$ and n, n' are integers while s labels the sites (resonators) of the system. W is the coupling matrix that describes the coupling between the propagating-channels (at the leads) and the system. Its matrix elements are $(W)_{n_P\alpha,n's} = \sqrt{v_{n_P}} c_\alpha \delta_{n_P n'} \delta_{\alpha\leftrightarrow s}$ where $v_{n_P} \equiv \partial\Omega/\partial k|_{k_{n_P}} = 2\sin k_{n_P}$ and the sub-index n_P labels only the propagating channels. The matrix $(W_c)_{n\alpha,n's} = c_\alpha \delta_{nn'} \delta_{\alpha\leftrightarrow s}$ and c_α describes the bare coupling between the lead α and the Floquet system where we define $\delta_{\alpha\leftrightarrow s} = 1$ when lead α is coupled with the site s directly or $\delta_{\alpha\leftrightarrow s} = 0$ otherwise. Finally the matrix K takes the form $(K)_{n\alpha,n'\alpha'} = \delta_{nn'} \delta_{\alpha\alpha'} \exp(\imath k_n)$.

We point out that our analysis involves scenarios for which strong non-Hermitian effects (like EPs etc) associated with the driving[44,50] are secondary as opposed to non-Hermiticity associated with material losses. Moreover, we assume that the material-related (non-radiative) losses are relatively weak and can be considered a small perturbation to the Hamiltonian of the isolated system. In such cases it is a standard practice to incorporate such effects to the diagonal part of $H(t)$ which in Eq. (1) is indicated as Γ. In this case the diagonal elements γ_μ can be obtained by estimating the shift of the imaginary part of the eigenfrequencies with respect to the lossless case, see Refs.[51,52].

III. NECESSARY CONDITIONS FOR DYNAMICALLY MODULATED PERFECT ABSORPTION

The scattering matrix $\mathcal{S}(\Omega_0, \gamma, \omega)$, Eq. (2), relates the incoming wave (in the propagating channel representation) $|\mathcal{I}\rangle$ to an outgoing wave $|\mathcal{O}\rangle$ emerging after the scattering with the periodically time-modulated target. In other words we have that $\mathcal{S}(\Omega_0, \gamma, \omega)\,|\mathcal{I}\rangle = |\mathcal{O}\rangle$. The condition for perfect absorption follows by requiring that the outgoing wave is the null vector, i.e. $|\mathcal{O}\rangle = 0$. The latter is satisfied for a set of *real valued* scattering parameters $(\Omega_{\rm DMPA}, \gamma_{\rm DMPA}, \omega_{\rm DMPA})$ for which $\det\left[\mathcal{S}\left(\Omega_{\rm DMPA}, \gamma_{\rm DMPA}, \omega_{\rm DMPA}\right)\right] = 0$. While the reality of the driving frequency ω and the loss-strength parameter γ are dictated by the formulation of the problem itself, the requirement for real incident frequencies $\Omega_0 = \Omega_{\rm DMPA}$ is based on physical considerations; namely the fact that the incoming wave has to be a propagating wave. Using Eq. (2) we are able to recast the above condition for DMPA to the following form

$$\det\left(\Omega_{DMPA} - H_Q + W_C^T K W_c - \imath W^T W\right) = 0 \qquad (3)$$

which resembles a generalized eigenvalue problem associated with an effective non-Hermitian Hamiltonian $H_{\rm eff} = H_Q - W_C^T K W_c + \imath W^T W$.

In the small coupling limit $c_\alpha \to 0$, a first-order perturbation approach allows us to evaluate theoretically $(\Omega_{DMPA}, \gamma_{DMPA})$ from Eq. (3)[53]. We have,

$$\Omega_{DMPA} \approx \Omega^{(0)} - \sum_{n_E,\alpha} c_\alpha^2 \left|\psi^{(0)}_{n_E s_\alpha}\right|^2 e^{\imath k^{(0)}_{n_E}} - \sum_{n_P,\alpha} c_\alpha^2 \left|\psi^{(0)}_{n_P s_\alpha}\right|^2 \cos k^{(0)}_{n_P}; \quad \gamma_{DMPA} \approx \sum_{n_P\alpha} c_\alpha^2 \left|\psi^{(0)}_{n_P,s_\alpha}\right|^2 \sin k^{(0)}_{n_P} \Big/ \sum_{n,\mu} \left|\psi^{(0)}_{n,\mu}\right|^2 \qquad (4)$$

where $\psi^{(0)}_{ns} = \langle e_{ns}\,|\psi^{(0)}\rangle$, $|e_{ns}\rangle$ is the unit vector in the Floquet-Hilbert space with the entry being $(|e_{n\mu}\rangle)_{n's} = \delta_{nn'}\delta_{\mu s}$ and $\left\{\Omega^{(0)}, |\psi^{(0)}\rangle\right\}$ is an eigenpair of the Hermitian matrix $H_Q(\gamma=0) = H_Q^\dagger(\gamma=0)$, i.e., $H_Q(\gamma=0)\,|\psi^{(0)}\rangle = \Omega^{(0)}\,|\psi^{(0)}\rangle$ and $\langle\psi^{(0)}\,|\psi^{(0)}\rangle = 1$. The index μ indicates the lossy resonators, n_E indicates the evanescent channels and n_P the propagating channels. Finally s_α labels the resonators which are coupled with the lead α directly, and $k^{(0)}_n$ is obtained from the dispersion $\Omega^{(0)}_n = \Omega^{(0)} + n\omega = -2\cos k^{(0)}_n$.

IV. COHERENT DMPA SCHEME

Equation (3), and its perturbative variant Eq. (4), are necessary conditions for PA. In case of multi-channel targets, however, one needs to impose an additional constraint; the incident waveform $|\mathcal{I}\rangle$ must be a linear combination of channel modes with amplitudes given by the components of the eigenvector $|\mathcal{I}_{\rm DMPA}\rangle$ of the scattering matrix Eq. (2) associated with a zero eigenvalue $s_{\rm DMPA}(\Omega_{\rm DMPA}, \gamma_{\rm DMPA}, \omega_{\rm DMPA}) = 0$. Such coherent incident waveform induces interference that trap the wave inside the structure, thus leading to a complete absorption. We refer to this scenario as Coherent DMPA.

As a useful illustration, we solve the DMPA problem explicitly in the case of one driven lossy resonator, i.e., $H_0(t) = h(t), h(t) \in R$, see Fig. 1a. Generally the eigenvectors $\left|\psi^{(0)}_n\right\rangle$ of the quasi-energy operator $H_Q(\gamma=0)$ are related to the Floquet mode associated with the Hamiltonian $H_0(t)$. In the case of one driven resonator, we can write the eigenvalues $\Omega^{(0)}_n$ and the corresponding eigenvectors $\left|\psi^{(0)}_n\right\rangle$ of $H_Q(\gamma=0)$ explicitly using the driving $h(t)$. Specifically, we have

$$\Omega^{(0)}_n = \Omega^{(0)} + n\omega, \quad \Omega^{(0)} = \frac{\omega}{2\pi}\int_0^{2\pi/\omega} dt\, h(t)$$
$$\langle n'\left|\psi^{(0)}_n\right\rangle = \frac{\omega}{2\pi}\int_0^{2\pi/\omega} dt e^{\imath(n'+n)\omega t} u(t) \qquad (5)$$

where $u(t) = \exp\left(-\imath\int_0^t dt' h(t') + \imath\Omega^{(0)} t\right) u(0)$ is the Floquet state of the time- periodic Hamiltonian $h(t)$ with the initial condition being $u(0)$.

In order to make further progress, we now consider a specific example where $h(t) = \beta\cos\omega t$. Using Eq. (5), we obtain $\Omega^{(0)}_n = n\omega$ and $\langle n'\left|\psi^{(0)}_n\right\rangle = J_{n'+n}(\beta/\omega)\,u(0)$, where $J_{n'+n}$ denotes the Bessel function of first kind of the integer order $n'+n$. Under the assumption that there exists only one propagating channel Ω in each lead, we get from Eq. (4)

$$\Omega_{DMPA} \approx 0, \; \gamma_{DMPA} \approx \left(c_L^2 + c_R^2\right) J_0^2(\beta/\omega) \qquad (6)$$

From Eq. (6), we see that due to the factor J_0^2, the lossy strength γ_{DMPA} required for the realization of DMPA

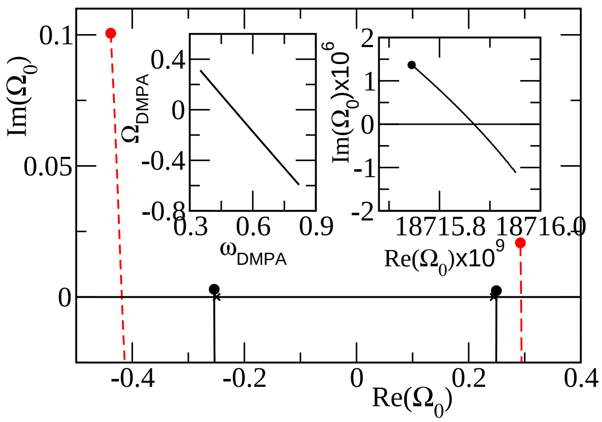

Figure 2: (Color Online) Parametric evolution of the zeros of the $\mathcal{S}$-matrix as the loss γ at one resonator of a network of four coupled resonators, increases (see Appendix A for the corresponding Hamiltonian and Fig. 1b for a mechanical analogue). The driving frequency is $\omega = 1$ and the amplitude is $\beta = 0.9$. The position of the zeroes for $\gamma = 0$ are indicated with filled circles. The two set of trajectories correspond to strong $c \approx -1$ (red-dashed lines) and weak $c \approx -0.2$ (black-solid lines) coupling of the resonators with the leads. The crosses indicate the predictions of perturbation theory Eq. (4). Right inset: The DMPA can be reconfigured to occur for an extremely small value of $\gamma_{\rm DMPA} \approx 2.76 \times 10^{-6}$ when the driving frequency is $\omega = 1$, and the driving amplitude is $\beta = 0.01$ ($c = -0.5$). Left inset: The Floquet network (with fixed topology and loss $\gamma = 0.0322$) can be reconfigured by changing the driving frequency ω and amplitude β in order to perfectly absorb an incident wave with a dense set of frequencies Ω_0. We show the numerically evaluated $\Omega_{\rm DMPA}$ versus $\omega_{\rm DMPA}$.

can be dramatically reduced. We refer to this phenomenon as Floquet-enhanced PA.

More complicated systems can be also used for the implementation of the coherent DMPA scheme. Take for example a network of coupled resonators or oscillators like the one shown schematically in Fig. 1b. This system consists of four coupled resonant modes with the central one having losses γ. For the numerical demonstration we have assumed that the coupling strength between the resonators can be modulated in a sinusoidal manner (the Hamiltonian $H(t)$ that describes the isolated driven system is given in the Appendix A). In Fig. 2 we report the parametric evolution of the complex zeroes of the scattering matrix found from Eq. (3) for two different sets of coupling constants. For $\gamma = 0$, the complex zeroes Ω are lying on the upper complex frequency semi-plane as a consequence of causality. When, however, $\gamma \neq 0$ these eigenvalues can, in principle, situated in both positive and negative half-planes of the complex frequency plane. The ones that have crossed the real axis at frequency $\Omega_{\rm DMPA}$ are relevant to our study, since for the corresponding loss-strength and/or driving frequency $\gamma_{\rm DMPA}, \omega_{\rm DMPA}$ (and driving amplitude β) an incident traveling waveform can be perfectly absorbed. In Fig. 2 we also mark with crosses (in the real Ω-axis) the theoretical predictions Eq. (4) associated to the case of weak coupling between the system and the leads. Furthermore, at the right inset of Fig. 2 we show the parametric evolution of the zeros in case that a Floquet-enhanced PA is engineered via a choice of appropriate frequency and amplitude of the modulated target. Specifically, for modulation frequency $\omega = 1$ and amplitude $\beta = 0.01$ we have observed a crossing of the zeros with the real axis which occurs for loss-strength as low as $\gamma = 2.7601 \times 10^{-6}$ (in coupling units).

An important element of our Dynamically Modulated Perfect Absorption protocol is the possibility to induce PA at different incident frequencies $\Omega_0 = \Omega_{\rm DMPA}$ without changing the fabrication characteristics of the cavity. Numerical evaluation of the secular Eq. (3) for an example case of a network of four coupled resonators (see Appendix A), indicates that these Floquet cavities can be reconfigured to act as PAs for a dense set of incident frequencies Ω_0 by simply changing the driving frequency $\omega = \omega_{\rm DMPA}$ (and driving amplitude β) of the coupling modulation, see left inset of Fig. 2. In fact, the reduced losses $\gamma_{DMPA} \approx 0.032$ (used in the left inset of Fig. 2) together with the relatively small driving amplitudes $\beta \approx 0.2$ and driving frequency $\omega_{DMPA} \sim 0.3$ (more than one order smaller than the band-width), opens up the possibility of achieving PA via the proposed DMPA scheme in the optical domain where one has to work with relatively slow modulation rates and amplitudes.

Let us finally comment on an alternative formulation that allows us to evaluate the coherent DMPA values $(\Omega_{\rm DMPA}, \gamma_{\rm DMPA})$ together with the corresponding incident waveform $|I_{DMPA}\rangle$. This approach involves the notion of the absorption matrix $A(\Omega, \gamma, \omega) \equiv I_{2N_p} - S^{\dagger}S = A^{\dagger}$. The eigenvalues $\alpha(\Omega, \gamma, \omega)$ of the absorption operator indicate the amount of absorption that a coherent incident waveform, with channel amplitudes dictated by the components of the associated eigenvector, will experience once it encounter the modulated target. Obviously the eigenvalues of the absorption operator are $0 \leq \alpha \leq 1$; when $\alpha(\Omega, \gamma) = 0$ the incident waveform is not absorbed, while $\alpha(\Omega = \Omega_{\rm DMPA}, \gamma = \gamma_{\rm DMPA}) = 1$ indicates complete absorption. Using Eq. (2), we can re-write the absorption matrix A in a simpler form

$$A = 2\gamma \sum_n \sum_\mu |u_{n\mu}\rangle \langle u_{n\mu}|, |u_{n\mu}\rangle \equiv W G_s^{\dagger} |e_{n\mu}\rangle. \quad (7)$$

In the weak-coupling limit and $\Omega_0 = \Omega_{DMPA}, \gamma = \gamma_{DMPA}$, we have $G_s \approx \langle \psi^{(0)} | G_s | \psi^{(0)} \rangle | \psi^{(0)} \rangle \langle \psi^{(0)} |$ and thus $|I_{DMPA}\rangle \propto W |\psi^{(0)}\rangle$. Therefore, the study of coherent DMPA in the weak-coupling limit boils down to the eigenvalue problem of the operator $H_Q\,(\gamma = 0)$.

V. DMPA BASED ON DYNAMICAL MIRRORS AND CRITICAL COUPLING

The implementation of PA protocols that do not need a coherent multi-sided illumination or a back-reflection mirror, is highly attractive for many applications and could open up many engineering possibilities. One way to achieve this goal is by utilizing the presence of accidental degeneracies of critically coupled modes with opposite symmetries[54] – a quite demanding scheme in terms of organizing appropriately resonant modes and their quality factors. Below we propose an altogether different approach which utilizes critical coupling to resonances. In this case, the physical back-reflection mirrors are absent and instead, we utilize appropriate Floquet driving schemes that generate *dynamical* mirrors.

The basic idea can be demonstrated using the simple system of Fig. 1c, described by the effective Hamiltonian Eq. (1) with

$$H_0\left(t\right)=\begin{pmatrix}\varepsilon_L & -e^{\imath\omega t}\\ -e^{-\imath\omega t} & \varepsilon_R\end{pmatrix} \text{ and } \Gamma=\begin{pmatrix}0 & 0\\ 0 & \gamma\end{pmatrix} \qquad (8)$$

due to a "right" lossy resonator. In the equation above $\varepsilon_{L/R}$ is the frequency of the left/right resonator respectively. To this end, we consider that an incident wave with frequency Ω_0, impinges the driven target from the left lead. The driving will couple the propagating channel Ω_0 only with the $\Omega_1=\Omega_0+\omega$ channel in the right lead[55]. To realize an DMPA in this framework, we consider Ω and ω values such that $\Omega_1>2$ (band edges) corresponding to an evanescent channel carrying zero flux. Essentially in this scenario, the Floquet scheme generates an impenetrable wall (dynamical mirror) at the right lead which enforces total reflection of the impinging wave. Consequently, the reflected wave exits the scattering domain at the same frequency Ω_0, as the incident wave. Using Eq. (2), we obtain the reflection amplitude (in case of perfect coupling $c=-1$)

$$r_0=-\frac{1-\left(\varepsilon_L+e^{\imath k_0}\right)\left(\varepsilon_R-\imath\gamma+e^{-\imath k_1}\right)}{1-\left(\varepsilon_L+e^{-\imath k_0}\right)\left(\varepsilon_R-\imath\gamma+e^{-\imath k_1}\right)}. \qquad (9)$$

Using Eq. (9) together with the DMPA condition $r_0=0$ we can evaluate the DMPA points $(\Omega_{\rm DMPA},\gamma_{\rm DMPA},\omega_{\rm DMPA})$.

For example, for an incident wave at frequency $E_0=E_{\rm DMPA}=0$ (middle of the band) we find that an DMPA occurs at loss strength $\gamma_{\rm DMPA}\approx 1/\varepsilon_L^2$ and driving frequency $\omega_{\rm DMPA}\approx 2\left(\varepsilon_R-\sqrt{\gamma_{\rm DMPA}}\right)$[56]. These DMPA points have a simple physical interpretation: In the limit of small losses $\gamma_{\rm DMPA}$, the on-site potential $\varepsilon_L\sim(1/\sqrt{\gamma})$ at the left site has to take large values. At the same time the Floquet driving creates a dynamical wall that forbids the incident wave to escape from the right lead. In other words, the scattering system turns to a high-Q cavity. When the incoming wave is at resonant with the modes of the cavity (i.e. perfect impedance matching) then it can be trapped for large times and eventually absorbed completely – even if the absorption strength γ is infinitesimally small. The above scenario is nothing else than the so-called impedance matching condition, which, once expressed in terms of losses, indeed states that radiative and material losses must be equal[57].

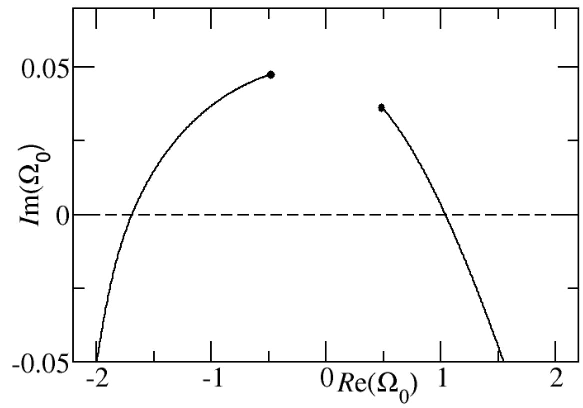

Figure 3: (Color Online) Parametric evolution (versus increasing driving amplitude β) of the zeros of the $\mathcal{S}$ matrix associated with a network of four fully connected resonators, two of which are coupled to leads (see Appendix B). The other two resonators have losses characterized by a loss-strength $\gamma=0.4749$ (fixed in these simulations). The driving frequency of the coupling is $\omega=5$ and the amplitude is increased from $\beta=0.15$ (indicated with filled circle) to $\beta=0.3$. The DMPA occurs for $\beta\approx 2.3$. This Floquet driving induces a dynamical mirror which can be used for PA via critical coupling.

The Floquet-induced critical coupling scenario of PA can be realized for more complicated cavities like a network of four fully connected resonators (see Fig. 1b). The model Hamiltonian that has been used in these simulations is shown in the Appendix B and assumes that two of the resonators have local losses γ. In Fig. 3 we show the parametric evolution of two of the complex zeroes of the scattering matrix $\mathcal{S}$ as the driving amplitude β increases. We find that there is an DMPA value at $\beta_{\rm DMPA}$ for a specific driving frequency $\omega_{\rm DMPA}$ and loss strength $\gamma_{\rm DMPA}$ for which the zeroes cross the real axis. We, therefore, conclude that at this real frequency an incident wave exists which is completely absorbed by the network.

VI. CONCLUSIONS

We have introduced a class of perfect absorbers that rely on Floquet engineering schemes. These Dynamically Modulated Perfect Absorbers (DMPA's) are easily reconfigurable, and can host a variety of new phenomena, including PA in the presence of infinitesimal local losses, and unidirectional reconfigurable PA's that operate without the use of physical mirrors. The latter are now substituted by dynamical (reconfigurable) mirrors realized using appropriate Floquet drivings schemes. Dynamically modulated PA's and other Floquet photonic systems is an emerging field which currently is in it's infancy. They can be proven useful in a variety of applications ranging from radar cloaking, sensing and photoexcitation control in photonic nanostructures, to linear optical switches, modulators, and coherence filtering of optical signals (for a review on potential applications see for example, Ref.[58]). Along these lines, promising future directions include the implementation of our DMPA's proposal in existing Floquet platforms (see for example[59]) and the implementation of DMPA protocols to realistic systems beyond the coupled mode theory approximation and under vectorial conditions. This will be the theme of future investigations.

Acknowledgements - This research was partially supported by DARPA NLM program via grant No. HR00111820042, by an AFOSR grant No. FA 9550-10-1-0433, and by an NSF grant EFMA-1641109. The views and opinions expressed in this paper are those of the authors and do not reflect the official policy or position of the U.S. Government.

Appendix A: Network system associated with Fig. 2

A network of coupled resonators has been used for the data shown in Figure 2. The network consists of four coupled resonators with time-modulated couplings (for a mechanical analog of such network see Fig. 1b). The corresponding isolated system is described by the following effective time-dependent Hamiltonian $H(t)$:

$$H(t) = \begin{pmatrix} 0 & -1+\beta\sin(\omega t) & -1+\beta\cos(\omega t) & -1+\beta\sin(\omega t) \\ -1+\beta\sin(\omega t) & 0 & -1+\beta\cos(\omega t) & -1+\beta\sin(\omega t) \\ -1+\beta\cos(\omega t) & -1+\beta\cos(\omega t) & -i\gamma & -1+\beta\cos(\omega t) \\ -1+\beta\sin(\omega t) & -1+\beta\sin(\omega t) & -1+\beta\cos(\omega t) & 0 \end{pmatrix} \tag{A1}$$

where we have assumed that there are two types of (out-of-phase) driving couplings $-1+\beta\sin(\omega t)$ and $-1+\beta\cos(\omega t)$.

In order to study the DMPA phenomena discussed in the main text, we have coupled this system with one-dimensional leads of coupled resonators. The left lead is coupled directly with the first site (resonator) while the right lead is directly coupled to the fourth site (resonator). Both (bare) couplings c are assumed to be equal. The loss, with loss-strength γ, has been included in the third resonator.

The data shown in the main panel of Fig. 2 correspond to the following parameters: $\omega = 1$, $\beta = 0.9$ for two different couplings $c = 1$ (strong coupling) and $c = 0.2$ (weak coupling). In this case the loss-strength γ was increasing in order to obtain the parametric evolution of the zeros of the $\mathcal{S}$ matrix.

The data associated with the right inset of Fig. 2 correspond to driving parameters ($\beta = 0.01; \omega = 1$) and coupling constant $c = 0.5$. Finally the data associated with the left inset of Fig. 2 correspond to $\gamma_{\rm DMPA} = 0.0322; c = 0.5$ and driving amplitude β ranging between $[0.1781, 0.472]$ with $\omega_{\rm DMPA}$ and $\Omega_{\rm DMPA}$ varying as shown.

Appendix B: Network system associated with Fig. 3

The results for Figure 3 are obtained when considering the time dependent Hamiltonian $H(t)$:

$$H(t) = \begin{pmatrix} 0 & \beta\cos(2\omega t) & \beta\cos(\omega t) & \beta\cos(3\omega t) \\ \beta\cos(2\omega t) & -i\gamma & \beta\cos(\omega t) & \beta\cos(\omega t) \\ \beta\cos(\omega t) & \beta\cos(\omega t) & -i\gamma & \beta\cos(2\omega t) \\ \beta\cos(3\omega t) & \beta\cos(\omega t) & \beta\cos(2\omega t) & 0 \end{pmatrix} \tag{B1}$$

where $\gamma = 0.4749, \omega = 5$ while the driving amplitude has been increased from $\beta =$0.15 to 0.3. The coupling to the leads is the same as the one used in the modeling for Fig. 2, with a coupling constant which is $c = 0.25$.

[1] C. M. Watts, X. Liu, W. J. Padilla, Adv. Lett. **24**, OP98 (2012).
[2] G. Dayal, S. A. Ramakrishna, Opt. Express **20**, 17503 (2012).
[3] Y. D. Chong, L. Ge, H. Cao, A. D. Stone, Phys. Rev. Lett. **105**, 053901 (2010).
[4] S. Longhi, Physics **3**, 61 (2010).
[5] W. Wan, Y. Chong, L. Ge, H. Noh, A. D. Stone, H. Cao, Science **331**, 889 (2011).
[6] Y. D. Chong, A. D. Stone, Phys. Rev. Lett. **107**, 163901 (2011).
[7] J. F. Zhang, K. F. Macdonald and N. I. Zheludev, Light: Science and Appl. **1**, 18 (2012).
[8] J. R. Piper, S. Fan, ACS Photonics **1**, 347 (2014).
[9] O. Kotlicki, J. Scheuer, Opt. Lett. **39**, 6624 (2014).
[10] M. L. Villinger, M. Bayat, L. N. Pye, A. Abouraddy, Opt. Lett. **40**, 5550 (2015).
[11] L. Baldacci, S. Zanotto, and A. Tredicucci, Rend. Fis. Acc. Lincei **26**, 219 (2015).
[12] B. C. P. Sturmberg, T. K. Chong, D-Y Choi, T. P. White, L. C. Botten, K. B. Dossou, C. G. Poulton, K. R. Catchpole, R. C. McPhedran, C. M. de Sterke, Optica **3**, 556 (2016).
[13] Y. Sun, W. Tan, H.-q. Li, J. Li, H. Chen, Phys. Rev. Lett. **112**, 143903 (2014).
[14] J. Slater, Microwave Electronics (Van Nostrand, Princeton,1950).
[15] N. I. Landy, S. Sajuyigbe, J. J. Mock, D. R. Smith, and W. J. Padilla, Phys. Rev. Lett. **100**, 207402 (2008).
[16] W. Padilla and X. Liu, SPIE Newsroom (2010), http://www.spie.org/newsroom/3137-perfect-electromagnetic-absorbersfrom-microwave-to-optical.
[17] V. T. Pham, J.W. Park, D. L. Vu, H. Y. Zheng, J. Y. Rhee, K.W. Kim, and Y. P. Lee, Adv. Nat. Sci. Nanosci. Nanotechnol. **4**, 015001 (2013).
[18] W. Dallenbach and W. Kleinsteuber, Hochfrequenztechnik und Elektroakustik **51**, 152 (1938).
[19] W.W. Salisbury, U.S. Patent No. 2,599,944, 10 June (1952).
[20] J. Mei, G. Ma, M. Yang, Z. Yang, W. Wen, and P. Sheng, Nat. Commun. **3**, 756 (2012).
[21] J. Z. Song, P. Bai, Z. H. Hang, and Y. Lai, New J. Phys. **16**, 033026 (2014).
[22] V. Romero-Garcia, G. Theocharis, O. Richoux, A. Merkel, V. Tournat, and V. Pagneux, Sci. Rep. **6**, 19519 (2016).
[23] G. Ma, M. Yang, S. Xiao, Z. Yang, P. Sheng, Nature Mater. **13**, 873 (2014).
[24] F. Costa, S. Genovesi, A. Monorchio, and G. Manara, IEEE Trans. Antennas Propag. **61**, 1201 (2013).
[25] Y. Pang, H. Cheng, Y. Zhou, and J. Wang, J. Appl. Phys. **113**, 114902 (2013).
[26] J. Schindler, Z. Lin, J. M. Lee, H. Ramezani, F. M. Ellis, and T. Kottos, J. Phys. A **45**, 444029 (2012).
[27] M. Law, L. Greene, J. Johnson, R. Saykally, P. Yang, Nat. Mater. **4**, 455 (2005).
[28] B. Tian, *et al.*, Nature (London) **449**, 885 (2007).
[29] H. A. Atwater, A. Polman, Nat. Mater. **9**, 205 (2010)
[30] M. Laroche, R. Carminati, J.-J. Greffet, J. Appl. Phys. **100**, 063704 (2006)
[31] A. Luque, S. Hegedus, *Handbook of Photovoltaic Science and Engineering* (Wiley, 2008).
[32] M. Fink, D. Cassereau, A. Derode, C. Prada, P. Roux, M. Tanter, J.-L. Thomas, F. Wu, *Time-reversed acoustics*, Rep. Prog. Phys. **63**, 1933 (2000)
[33] L. Borcea, G. Papanicolaou, C. Tsogka, J. Berryman, *Imaging and time reversal in random media*, Inverse Probl. **18**, 1247 (2002).
[34] G. Montaldo, P. Roux, A. Derode, C. Negreira, M. Fink, *Ultrasound shock wave generator with one-bit time reversal in a dispersive medium, application to lithotripsy*, Appl. Phys. Lett. **80**, 897 (2002).
[35] J. Dela Cruz, I. Pastirk, M. Comstock, V. Lozovoy, M. Dantus, *Use of coherent control methods through scattering biological tissue to achieve functional imaging*, Proc. Natl Acad. Sci. USA **101**, 17001 (2004).
[36] R. Horstmeyer, H. Ruan, C. Yang, *Guidestar-assisted wavefront-shaping methods for focusing light into biological tissue* , Nat. Photonics **9**, 563 (2015).
[37] R. L. Fante, M. T. McCormack, IEEE Trans. Ant. Prop. **36**, 1443 (1998)
[38] K. Vinoy, R. Jha, *Radar absorbing materials - From theory to design and characterization* (Kluwer Academic Publishers, 1996).
[39] J. Mei, *et al.* Nature Communications **3**, 756 (2012).
[40] H. Zhao, W. S. Fegadolli, J. Yu, Z. Zhang, L. Ge, A. Scherer, L. Feng, Phys. Rev. Lett. **117**, 193901 (2016)
[41] H. Li, S. Suwunnarat, R. Fleischmann, H. Schanz, T. Kottos, Phys. Rev. Lett. **118**, 044101 (2017).
[42] Y. V. Fyodorov, S. Suwunnarat, T. Kottos, J. Phys. A: Math. Theor. **50**, 30LT01 (2017).
[43] H. Li, S. Suwunnarat, T. Kottos, Phys. Rev. B **98**, 041107 (2018).
[44] T. T. Koutserimpas, A. Alú, R. Fleury, Phys. Rev. A **97**, 013839 (2018).
[45] Z. Yu, S. Fan, Nat. Phot. **3**, 91 (2009)
[46] R. Fleury, D. Sounas, M. R. Haberman, and A. Alu, Acoust. Today **11**, 14 (2015).
[47] C. Caloz, A. Alu, S. Tretyakov, D. Sounas, K. Achouri, Z-L Deck-Leger, Phys. Rev. Applied **10**, 047001 (2018).
[48] H. Li, T. Kottos, and B. Shapiro, Phys. Rev. Applied **9**, 044031 (2018).
[49] H. M.Pastawski, Physica B: Condensed Matter **398**, 278 (2007)
[50] N. Wang, Z-Q Zhang, C. T. Chan, Phys. Rev. B **98**, 085142 (2018).
[51] F. Alpeggiani, N. Parappurath, E. Verhagen, and L. Kuipers, Phys. Rev. X 7, 021035 (2017).
[52] H.-J. Stökmann, Quantum Chaos: An Introduction (Cambridge University Press, Cambridge, England, 1999).
[53] We assume a fixed driving scheme (i.e. frequency and modulation) and solve for the corresponding $(E_{\rm DMPA}, \gamma_{\rm DMPA})$. Of course the calculations can be also performed assuming γ fixed and identifying the set $(E_{\rm DMPA}, \omega_{\rm DMPA})$ for which PA occurs.
[54] J. R. Piper, V. Liu, S. Fan, Appl. Phys. Lett. **104**, 251110 (2014)
[55] H. Li, T. Kottos, and B. Shapiro, Phys. Rev. A **97**, 023846 (2018).
[56] In the calculation we assumed a scenario for which the driving frequency ω is slightly larger than 2 and thus $e^{-\imath k_1} \approx -\omega/2$.
[57] H.A. Haus, Waves and fields in optoelectronics (Prentice-

Hall, Englewood Cliffs, NJ, 1984)
[58] D. G. Baranov, A. Krasnok, T. Shegai, A. Alú, Y. Chong, Nature Reviews **2**, 17064 (2017)
[59] M. Chitsazi, H. Li, F. M. Ellis, T. Kottos, Physical Review Letters **119**, 093901 (2017)